Mekanika: Majalah Ilmiah Mekanika

Hydrodynamic Performance Assessment of Straight and Helical Hydrokinetic Turbine Hydrofoil-Blade Sections in River Oyun, North-Central Nigeria

Laniyi Laniran Ladokun[1*]

1 Department of Turbo-Machines Design and Construction, University of Ilorin, Ilorin, Nigeria

*Corresponding Author's email address: ladokunll.nachred@unilorin.edu.ng

Keywords:
Hydrokinetic
Straight-blade
Helical-blade
Coefficient of performance
Tip speed ratio

Abstract
The performance of lift-based hydrokinetic rotor turbines usually depends on the blade sections or hydrofoil profile. Different hydrofoil blade sections, having different profiles and geometries, give different coefficients of performance in different hydrodynamic settings. This study examined the influence of blade geometry on the power stage characterization of vertical axis crossflow hydrokinetic turbines under conditions of low river current velocity. Two turbines have been selected to characterize the power stage. Pre-developed straight-bladed National Advisory Committee for Aeronautics (NACA) 0021 hydrofoil blade sections and a Gorlov helical/curved NACA 0021 pattern were used in the hydrodynamic experimental characterization along River Oyun, Kwara State, North-Central Nigeria. The graphical ratio of the coefficient of performance, $C_{P,}$ which measures the efficiency of the turbine blade sections converting kinetic energy into mechanical energy, and the turbine blade Tip Speed Ratio (TSR), was used to analyze the hydrodynamic blade performance characterization. The peak C_P values, the optimal TSR, the C_P curve shape, and the stall regions from the C_P-TSR chart were used to determine the hydrofoil with optimal performance.

1 Introduction

Hydro energy converters, which extract energy from marine currents in natural streams, rivers, or constructed waterways, are a promising avenue for renewable energy. These devices, which utilize the power of moving water to turn turbines placed directly in domestic rivers, estuaries, coastal waters, or tidal flows, have the potential to significantly contribute to the renewable energy landscape [1-5]. The turbines are usually placed underwater, in a fixed, floating, anchored, or towed configuration, and in any location where the effective water current preferably flows with a minimum speed of about 0.25 m/s [6]. Hydrokinetic turbine systems, which provide a sustainable alternative for extracting energy from free-flowing water, are an exciting area of research. The specially shaped hydrofoils, which are part of the turbine blade, are designed to generate a lift force when the turbine moves through flowing water, thereby increasing the hydrodynamic performance of the turbine [7,8].

https://dx.doi.org/10.20961/mekanika.v23i2.92527

Revised 17 September 2024; received in revised version 20 September 2024; Accepted 22 October 2024
Available Online 23 October 2024

2579-3144

Therefore, the performance of lift-based hydrokinetic rotor turbines is usually dependent on the profile of the hydrofoil used [9,10]. Darrieus turbines are a class of turbines that base their operation on the lift force generated when the difference in pressure between the blades produces a rotational movement, thus achieving optimal operational performance. There are several modifications in the design and configurations of this type of rotor. An example is the H-Darrieus turbine, which consists of vertical blades attached to the shaft using horizontal supports. An improved variant is the squirrel cage-Darrieus rotor. This system is composed of two discs located at the top and bottom of the device that serve as support for the blades that are arranged vertically [11].

A helical-bladed vertical-axis hydrokinetic turbine is a crossflow type turbine that rotates in a fixed direction irrespective of the water current direction when the axis of rotation is at right angles to the flow path. It does not need any yaw control device to point the turbine in the flow direction [12]. One of the advantages of the helical-bladed turbine is that it improves the self-starting ability of the turbine compared to a straight-bladed turbine [13]. Since the helical blade shape sweeps along the circumference of the rotation of the turbine, some portion of the blade profile is always located at the optimum angle of attack, even in static or slowly rotating conditions. This produces more uniform starting torque and less dependency upon turbine azimuthal position [14,15]. Studies have been done to investigate a suitable blade geometry for optimal hydrokinetic performance [7,16-19].

The lift, drag, and pressure coefficients of various hydrofoils from the National Advisory Committee for Aeronautics (NACA), the National Renewable Energy Laboratory (NREL), and the Risø National Laboratory for Sustainable Energy were studied by [6] to investigate the lift/drag ratio. However, the C_P-TSR tool as a means of hydrodynamic analysis was not considered. The experimental study of two candidate hydrofoils was done by [16] using a hydrodynamic tunnel and a high-precision torque meter. The study of [17] investigates the effects of blade number and solidity on the performance and wake recovery of a small-scale vertical axis helical hydrokinetic turbine under different tip speed ratios and inflow velocities using Computational Fluid Dynamics (CFD) simulations. Likewise, [18] studied the development and performance characterization of a hydrokinetic turbine using a NACA 0020 bladed vertical-axis turbine with a solidity ratio of 0.38 and an aspect ratio of 1.0. Experiments were carried out at an irrigation sluice with a water velocity of 1.1 m/s. It was observed that the developed helical-bladed turbine demonstrates a peak power coefficient of 0.16 at a tip-speed ratio of 0.85. Standard airfoils, like NACA and Gottingen, were studied by Yavuz and Koç [19] for wind and hydrokinetic turbines using CFD. Using double-blade airfoil, minimum wind and hydrokinetic flow velocities that shall produce economic energies at 3-4 m/s for wind turbines and 1-1.5 m/s or less for hydrokinetic turbines were obtained, which could redefine the energy industry. This study investigated the influence of blade geometry on the power stage characterization and performance of the NACA 0021 straight-bladed turbine profile and the NACA 0021 helical turbine blade under conditions of low current velocity.

2 Experimental Methods

The hydrofoil geometric patterns are:

a) NACA 0021 straight-bladed fixed pitch turbine rotor blade

b) NACA 0021 helical (curved) turbine rotor blade

The experimental method used for the study is presented in Figure 1. The outlines of the candidate hydrofoils were developed using CAD software, and models were fabricated using specially selected materials. Riverine tests were carried out, and measurements were taken, which were used for computations and analysis. The method involved a series of steps, including hydrofoil design, model fabrication, riverine testing, and data analysis.

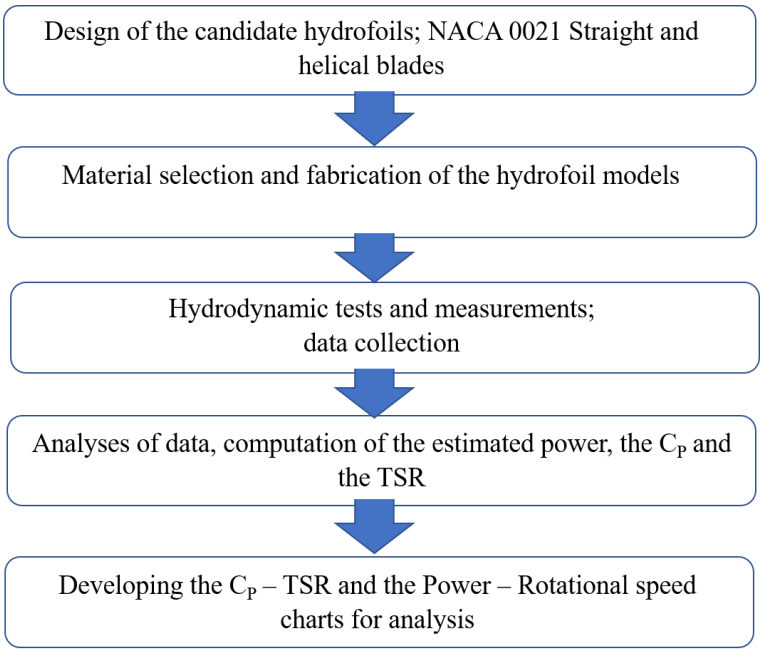

Figure 1. Flowchart of the experimental method in analyzing the C_P–TSR of the hydrofoils

2.1 NACA 0021 hydrofoil

The NACA 0021 foil shown in Figure 2 is one of the NACA four-digit section series. It is a 21% thick, symmetrical airfoil with the point of maximum thickness located at x/c = 0.30, where x is the axial coordinate measured from the airfoil's nose, and c is the chord length. The 00 indicates that it has no camber. The hydrodynamic properties, such as its thickness, camber, and trailing edge angle, are crucial in determining its performance in hydrokinetic turbines and are listed in Table 1.

Figure 2. The NACA 0021 hydrofoil

Table 1. The hydrodynamic properties of NACA 0021

Hydrodynamic Property	Value	Hydrodynamic Property	Value
Thickness	20.9%	Max. C_L	1.197
Camber	0.0%	Max. C_L angle	15.0
Trailing edge angle	35.9%	Max. L/D	28.271
Lower flatness	3.8%	Max. L/D angle	8.5
Leading edge radius	5.9%	Stall angle	4.5
Efficiency / C_P	47.6	Zero-lift angle	0.0

2.2 The NACA 0021 straight-bladed crossflow, vertical axis turbine

The first turbine shown in Figure 3 is a variant of the H-Darrieus turbine with flat metallic plates at the ends like the Darrieus Squirrel Cage (SC-Darrieus)-type rotor. It comprises six straight blades of

standard NACA 0021 profile, which are spaced 60 degrees apart and whose dimensions are specified in Table 2. The turbine also has a system of nuts and threads for joining the rotor struts to the diameter metal shaft, which facilitates interchangeability between different types of turbines. The length of the shaft is 0.865 m and is hollow and concentric to allow for lightness while not compromising the strength.

2.3 The NACA 0021 helical-shaped crossflow, vertical axis turbine

The other turbine to be used for testing will be a Gorlov-type helical-shaped crossflow, vertical axis turbine with six NACA 0021 type blades at 45° angle of rotation and spaced 60° apart, whose measurements are also specified in Table 2. It also has a system of nuts and threads for coupling the helical blades to the turbine struts. The length of the shaft is also 0.865 m. Figure 4 presents a typical helical-shaped hydrokinetic turbine.

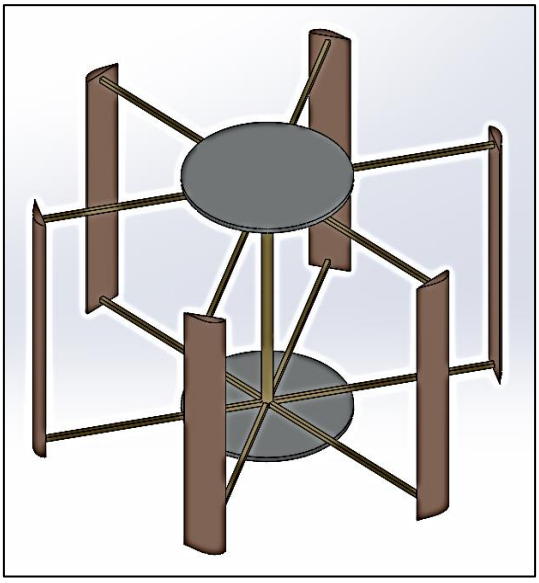

Figure 3. Straight-bladed hydrokinetic turbine

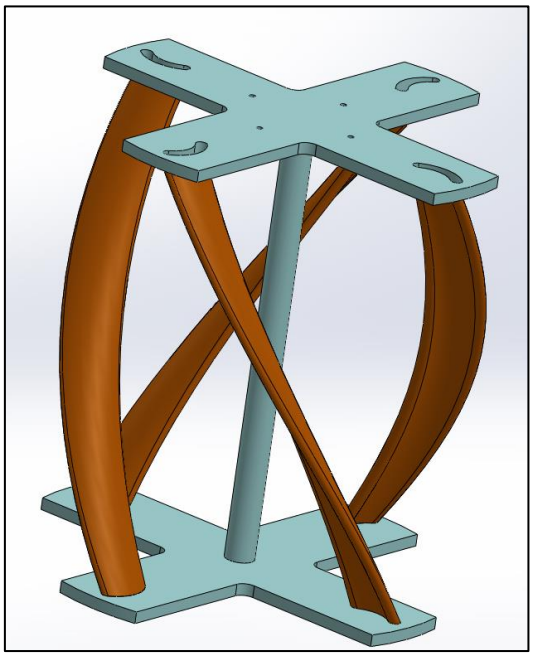

Figure 4. Helical-bladed hydrokinetic turbine

Table 2. Turbine dimensions

Hydrokinetic Turbine Geometry	Number of Blades	Hydrofoil Profile	Chord (m)	Height (m)	Diameter (m)
Straight blade Crossflow Hydrokinetic	6	NACA 0021	0.09144	0.4527	0.5052
Helical Crossflow Hydrokinetic	6	NACA 0021	0.09144	0.5026	0.5052

3 Construction and Experimental Testing of Turbine Hydrofoil Geometries

3.1 Selected study site

River Oyun flows through the University of Ilorin, from the state's southeastern part, and through the Oyun dam in Offa, Kwara State. Oyun River Basin is located in the south-eastern part of Kwara State between longitudes 4°38'E and 4°03'E and latitudes 9°50'N and 8°24'N. The total area of the Oyun River Basin is about 452.80 km^2, while the total perimeter is 191.5/km^2. The field tests were conducted in a controlled area with a high Reynolds number quasi-laminar flow on the lee (downstream) of a hump which was characterized by reduced turbulence intensity, smaller eddies and vortices, and increased coherence and organization. The Reynolds number of the flow was 14,970,059.9. The site was selected due to its easy accessibility, large channel, available volume of water (high discharge), considerable flow velocity, weedless and relatively smooth riverbed, and moderate water temperature. The free stream velocity of the river, the induced velocity at the turbine hydrofoil, and the wake velocity were obtained through direct measurements using hydro-mechanical instruments and empirical correlations.

3.2 Hydrofoil material selection

For this research, experimental tests were carried out on scale models of the two crossflow turbine hydrofoil patterns in a controlled riverine environment. The hydrofoil profiles were developed and machined into the turbine blades. The material used for the construction was Nigerian teak, which is locally called ara wood (a local wooden species peculiar to northern Kwara State, North-Central Nigeria). Table 3 presents the features and specifications of the Nigerian Teak wood [20].

Table 3. Features and specifications of the Nigerian Teak wood [20]

Features	Specifications	Features	Specifications
Common name	Nigerian Teak	Av. Dried Weight	655 kg/m^3
Scientific name	*Tectona Grandis*	Specific gravity	0.55
Distribution	South Africa, Southeast Asia, South America	Janka Hardness	4,740 N
Elastic modulus	12.28 GPa	Modulus of Rupture	97.1 MPa

3.3 Evaluation of rotor performance

The revolutions per minute of the candidate hydrofoils were also measured at specific depths to obtain their tangential velocities. Power from a hydrokinetic device can be expressed in Equation 1.

$$P = \frac{1}{2}\rho A {U_0}^3 \eta Cp \quad (1)$$

Where ρ is the mass density in kg/m^3, A is the swept area of the rotor blade in m^2, U_0 is the velocity of the fluid in m/s, η is the generator's efficiency, and C_P is the power coefficient. The Power Coefficient (C_P) is the ratio between the available energy and the energy that is finally generated, see Equation 2.

$$C_p = \frac{P_{available}}{P_{generated}} \quad (2)$$

To determine the operating efficiencies of the turbine, it is necessary to obtain the relationship between the C_P and the relative speed at the tip of the turbine blade. This is referred to as the Tip Speed Ratio (TSR) for hydrokinetic turbines and is defined as the ratio between the rotational speed of the tip of a blade and the actual velocity of flow of the water, as shown in Equation 3.

$$\lambda = \frac{V_{tangential}}{V_\infty} = \frac{\omega R}{V_\infty} \quad (3)$$

where TSR is the Tip Speed Ratio, ω is the rotational speed in rad/s, R is the turbine radius (m), and v is the current velocity at the blade tip (m/s)

The power (in Watts) generated by the hydrofoils was used to compute the power coefficient. The performance of the candidate hydrofoils was compared based on the power coefficients and the tip speed ratio (C_P-TSR) plots. Power coefficients were calculated using the single tube design model and the blade-element-momentum theory method. Figure 5 presents plates evaluating some of the hydrofoils in a controlled riverine environment.

Figure 5. Evaluation of the hydrokinetic geometries in a controlled riverine environment

The river flow velocity was measured using the global water flow probe. The water velocity probe consists of a protected water turbo prop positive displacement sensor and an expandable probe handle ending in a digital readout display. The water flow meter incorporates actual velocity averaging for accurate flow measurements. It can record and store 30 data sets. Figure 6 (a) presents the Flow probe, 6 (b) presents the digital readout display, and 6 (c) the turboprop displacement sensor. The rotational velocity of the turbine was also measured during experimental testing. Rotational velocity was measured in units of revolutions per minute (rpm) using a digital tachometer, shown in Figure 7. The operational range of this instrument is 1 to 99,999 rpm and is accurate to ±0.02%.

(a) (b) (c)

Figure 6. Global flow probe

Figure 7. Digital tachometer

4 Results and Discussion

The charts for the hydrokinetic blade geometries are presented (Figures 8 and 9). Figure 8 shows the diagram of power against blade speed in revolutions per minute and that of the coefficient of power (C_P) versus the tip speed ratio for the straight blade NACA 0021 hydrokinetic rotor profile, which determines the performance of the turbines. The power coefficients were obtained from the turbine power ratio to the water's available power. As can be seen, as the water current speed increased, the mechanical power of the rotor also increased. Peak power of 94.676 W was obtained at a flow velocity of 1.25 m/s. From the curve, an optimal water velocity of 1.56 m/s for the NACA 0021 gave 45.194 W. By applying the dimensionless TSR and C_P coefficients, a first approximation of the straight-type NACA 0021 rotor performance was obtained. It is observed that, for the various water current velocities, the rotor reached CP values of 0.22 at a TSR of 0.89, which could infer an optimal performance of the hydrofoil to lift.

Figure 9 presents the outcomes obtained from the evaluation of the NACA 0021 helical-type rotor under the same hydrodynamic conditions as the straight-bladed rotor. In this case, the rotational speeds of the turbine were very similar to those of the straight-bladed rotor as they reached 0.89 TSR. However, for the water speed test, the helical turbine obtained a higher power of ≈ 1430.62 W. Similarly, the dimensionless parameters TSR and C_P were obtained for the helical-type rotor. In this case, there has been an increase in the maximum values of TSR and C_P compared to those obtained with the straight blade-type rotor. More specifically, a maximum value of C_P of 0.533 has been reached for a TSR of 1.385. The above results compare favorably with those obtained from the hydrodynamic tunnel tests of [16] using two similar candidate hydrofoils.

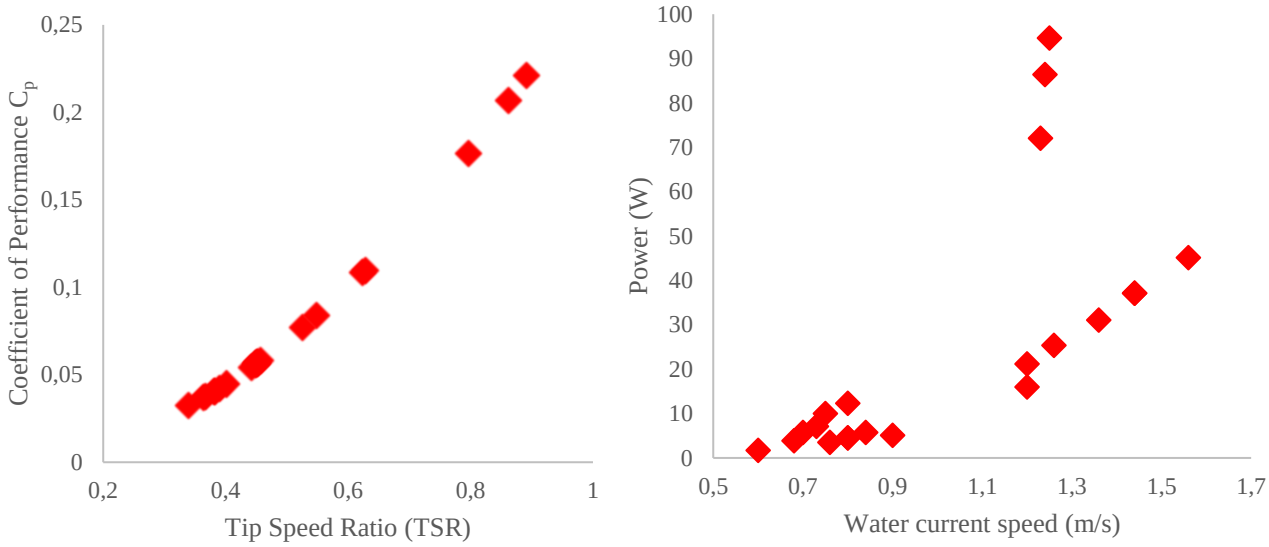

(a) (b)

Figure 8. Chart for NACA 0021 straight blade turbine (a) C_P–TSR curve, and (b) Power–Rotor speed curve

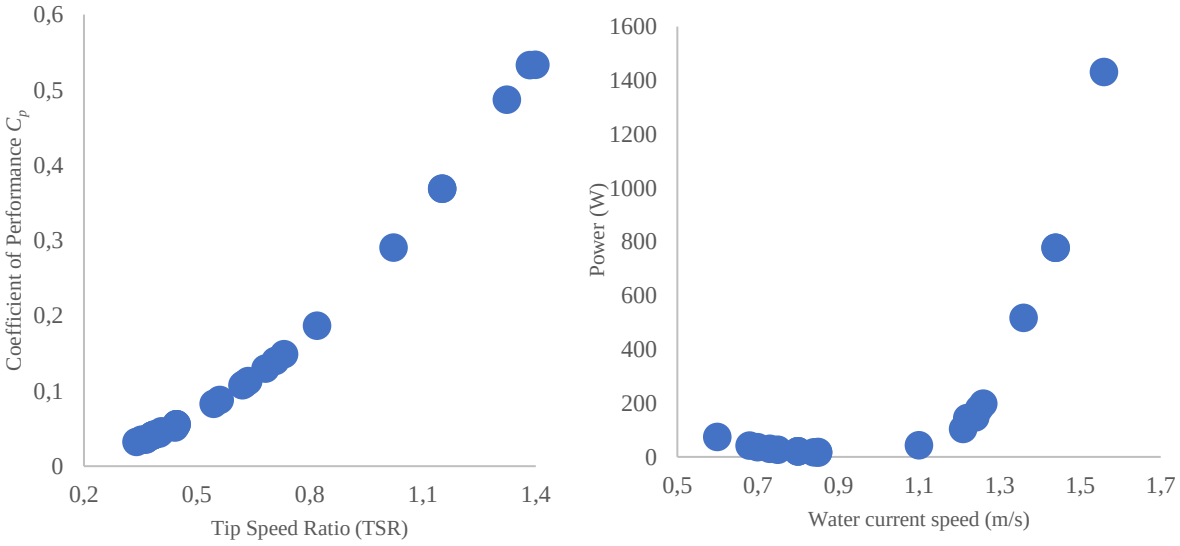

(a) (b)

Figure 9. Chart for NACA 0021 helical blade turbine: (a) C_P–TSR curve, and (b) Power–Rotor speed curve

A combined C_P-TSR curve is presented in Figure 10, which compares the coefficient of power (C_P) for the two hydrofoil rotor geometries, which determines the performance of the turbines. As can be observed from the chart, the helical-bladed turbine geometry achieved higher C_P than the straight-blade turbine for the corresponding TSR. Figure 11 presents the power versus water current speed chart for the two turbine blade geometries. At low water current speed, the helical turbine delivered equivalent power with the straight blade until the water current crossed the 1 m/s mark. The helical turbine power curve went exponentially, showing that at water speeds beyond 1 m/s, the helical turbine obtained higher power than the straight-blade turbine.

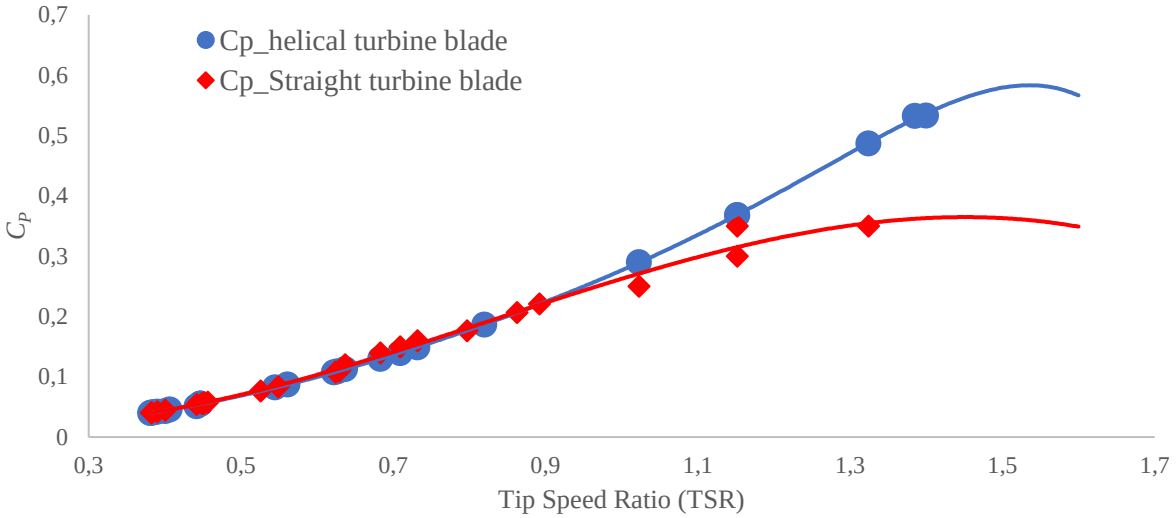

Figure 10. C_P vs TSR for straight-bladed turbine and helical turbine

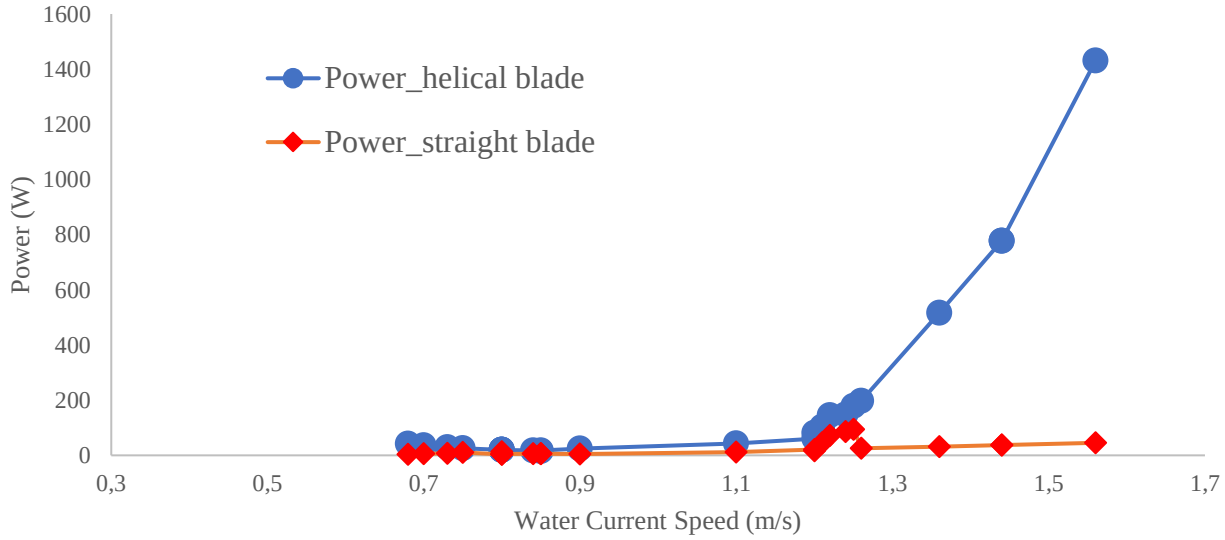

Figure11. Power–rotor speed for straight-bladed turbine and helical turbine

5 Conclusions

The performance of NACA 0021 hydrokinetic blade geometries at relatively low water current speeds has been analyzed. A crossflow straight blade Darrieus turbine and a cross-flow helical blade Darrieus turbine with identical dimensions and solidity were evaluated at similar velocities and flow conditions. The results obtained from the controlled riverine experimental study showed that the NACA 0021 helical turbine achieved an optimal C_P of 0.533, higher than that of the NACA 0021 straight blade geometry of 0.22 and at a higher TSR of 1.385 for the helical as compared with the 0.89 of the straight blades. Also, the helical turbine obtained greater power (≈ 1.43 kW) than the straight-blade rotor (0.0452 kW) at a similar water speed. Therefore, the NACA 0021 helical hydrokinetic turbine is more suitable for deployment for power generation than the NACA 0021 straight-bladed turbine when crossflow turbines are to be considered. However, further work on improving the C_P values compared to axial turbines and obtaining higher efficiencies at high TSR could be looked into.

References

1. M. J. Khan, M. T. Iqbal, and J. E. Quaicoe, “River current energy conversion systems: Progress, prospects and challenges,” *Renew. Sustain. Energy Rev.*, vol. 12, no. 8, pp. 2177-2193, 2008.

2. L. I. Lago, F. L. Ponta, and L. Chen, “Advances and trends in hydrokinetic turbine systems,” *Energy Sustain. Dev.*, vol. 14, no. 4, pp. 287-296, 2010.
3. C. A. Cuenca, A. S. Barzola, B. E. Carriel, and R. J. Paredes, "Hydrokinetic turbines, an alternative for the transformation of the Agro-Industrial sector", *E3S Web Conf.*, vol. 532, article no. 02003, 2024.
4. P. Jacobson, *Hydrokinetic power could provide 3% of annual US power demand, says EPRI*, Dartford: International Water Power and Dam Construction. Available in https://www.waterpowermagazine.com/news/hydrokinetic-power-could-provide-3-of-annual-us-power-demand-says-epri/(Accessed in August 8, 2024).
5. B. Muhando, G. Holdmann, M. Mager, and K. Keith, “Alaska Center for Energy and Power,” *Alaska Cent. Energy Power*, pp. 1-4, 2019.
6. M. J. Khan, G. Bhuyan, M. T. Iqbal, and J. E. Quaicoe, “Hydrokinetic energy conversion systems and assessment of horizontal and vertical axis turbines for river and tidal applications: A technology status review,” *Appl. Energy*, vol. 86, no. 10, pp. 1823-1835, 2009.
7. A. Muratoglu and M. I. Yuce, “Performance analysis of hydrokinetic turbine blade sections,” *Adv. Renew. Energy*, vol. 2, pp. 1-10, 2015.
8. M. Anyi and B. Kirke, “Hydrokinetic turbine blades: Design and local construction techniques for remote communities,” *Energy Sustain. Dev.*, vol. 15, no. 3, pp. 223-230, 2011.
9. S. Subhra Mukherji, N. Kolekar, A. Banerjee, and R. Mishra, “Numerical investigation and evaluation of optimum hydrodynamic performance of a horizontal axis hydrokinetic turbine,” *J. Renew. Sustain. Energy*, vol. 3, no. 6, article no. 063105, 2011.
10. S. S. Mukherji, *Design and critical performance evaluation of horizontal axis hydrokinetic turbines*, Missouri: Missouri University of Science and Technology, 2010.
11. D. G. J. Marie, "Turbine having its rotating shaft transverse to the flow of the current," US Patents, no. US-1835018-A, 1931.
12. P. K. Talukdar, V. Kulkarni, and U. K. Saha, “Field-testing of model helical-bladed hydrokinetic turbines for small-scale power generation,” *Renew. Energy*, vol. 127, pp. 158-167, 2018.
13. M. Shiono, K. Suzuki, and S. Kiho, “Output characteristics of Darrieus water turbine with helical blades for tidal current generations,” in *ISOPE International Ocean and Polar Engineering Conference*, Kitakyushu, Japan, 2002.
14. A. Gorlov, *Development of the helical reaction hydraulic turbine. Final technical report, July 1, 1996--June 30, 1998*, Boston: Northeastern University, 1998.
15. P. K. Talukdar, S. Kumar, V. Kulkarni, A. K. Das, and U. K. Saha, “On site testing of a zero head vertical axis helical water turbine for power generation,” *ASME 2015 Gas Turbine India Conference*, vol. 57311, article no. V001T11A001, 2015.
16. R. E. Valdés, A. G. Yosry, R. Ferraiuolo, A. F. Jiménez, and V. M. F. Pacheco, “Experimental Comparison between Hydrokinetic Turbines: Darrieus vs. Gorlov,” *Environ. Sci. Proc.*, vol. 21, no. 1, article no. 26, 2022.
17. K. B. Reddy and A. C. Bhosale, “Effect of number of blades on performance and wake recovery for a vertical axis helical hydrokinetic turbine,” *Energy*, vol. 299, article no. 131520, 2024.
18. P. K. Talukdar, V. Kulkarni, D. Dehingia, and U. K. Saha, “Evaluation of a model helical bladed hydrokinetic turbine characteristics from in-situ experiments,” *ASME 2017 11th International Conference on Energy Sustainability*, vol. 57595, article no. V001T07A005, 2017.
19. T. Yavuz and E. Koç, “Performance analysis of double blade airfoil for hydrokinetic turbine applications,” *Energy Convers. Manag.*, vol. 63, pp. 95-100, 2012.
20. Wood Assistant, *Teak - Characteristics and Uses of Teak Wood*. Available in http://www.woodassistant.com/wood-database/teak/(Accessed in August 4, 2024).